Pramāṇa – J. Phys., Vol. 25, No. 1, July 1985, pp. 63–70. © Printed in India.

# Effect of lateral energy transport on ablation pressure scaling in laser irradiated planar foil targets

L J DHARESHWAR, P A NAIK, S SHARMA and H C PANT
Laser Division, Bhabha Atomic Research Centre, Bombay 400085, India

MS received 26 November 1984

**Abstract.** Experimental investigations on ablatively accelerated thin plastic foil targets irradiated by a 6J, 5 nsec Nd : glass laser pulse, were conducted using shadowgraphy technique. A 2 nsec, 0·53 $\mu$m probe pulse, derived from the main laser was used for recording the foil motion. It was observed that 6 $\mu$m plastic foils could be accelerated to a velocity of about $3 \times 10^6$ cm/sec for an incident laser intensity of $5 \times 10^{13}$ W/cm$^2$ and the corresponding ablation pressure was 0·4 Mbar. Ablation pressure ($P$) scaling against absorbed laser intensity ($I_a$) was slower ($P \propto I_a^{0.4}$) for a smaller laser focal spot (30 $\mu$m) as compared to the scaling ($P \propto I_a^{0.7}$) for a larger focal spot (500 $\mu$m). This result has been explained considering the loss due to lateral energy transport from the laser plasma interaction region.

**Keywords.** Plasma; laser fusion; ablative compression; shadowgraphy; lateral transport.

**PACS No.** 52·25; 52·50; 52·70

## 1. Introduction

One of the prerequisites to achieve compression of laser fusion targets to high densities is to produce high and uniform ablation pressure (Nuckolls *et al* 1972; Bruckner and Jorna 1974). One has to however, optimise the incident laser intensity for efficient compression of fusion targets. High irradiance laser pulses in principle can produce high ablation pressures. However, very high laser irradiance is known to generate non-thermal effects which inhibit efficient target compression. One of the alternatives then, is to use a longer (nsec) duration pulse with moderate irradiance of about $10^{14}$ W/cm$^2$. Compression studies of spherical pellets is of current interest; however, to simplify the experiments, planar foil targets are also used. In planar foil targets, the interaction area can be considered to model a small section of a hollow spherical pellet. This not only affords interpretational simplicity but also provides an access to the rear side of the target. In experiments such as preheat studies, this is of utmost importance. It has, however, been observed that the ablation pressure achievable in plane target experiments with sharply focussed, intense laser beams are overestimated by idealised plane computer simulations (Van Kessel 1975). This happens due to reduction of the effective laser intensity by lateral transport losses (Nishimura *et al* 1981; Lewis *et al* 1982). Lateral transport causes target ablation over an area much larger than that heated directly by the laser beam. By lateral transport, we mean the transport of energy from the laser focal spot region to regions not directly heated by the laser beam. The

effective intensity ($I_{eff}$) due to lateral transport can be expressed as $I_{eff} = I/(D_a/D_f)^2$ where $I$, $D_a$ and $D_f$ are respectively the incident laser intensity, diameter of the ablated region of the target and the original laser focal spot diameter. The periphery of the ablated region spreads due to lateral transport. The extent of this spreading depends on the plasma temperature which in turn varies with laser intensity. The fractional increase in the ablation diameter reduces with increase in the laser focal spot size at the target. Since lateral transport decreases with larger laser focal spot diameters, the only way to avoid reduction in ablation pressure is to keep the laser spot diameter large (Grun *et al* 1982; Pant *et al* 1984; Ripin *et al* 1980). Although earlier authors have discussed the effects of lateral energy transport, its effects through laser spot size on ablation pressure scaling has not been reported.

In this paper, we report that the ablation pressure scaling with laser irradiance is affected by the beam focussing conditions. Higher ablation pressures are obtained for a larger spot irradiation for a given laser intensity. In the experiments described here, optical shadowgraphy technique was used for recording the motion of the laser irradiated foil targets. Ablation pressure was estimated by measuring target velocity. This technique has been widely used in other laboratories as well (Grun *et al* 1982; Ripin *et al* 1980; Raven *et al* 1982).

## 2. Experiments

In the experiments described here, a single Nd: glass laser beam delivering 6J energy in a 5 nsec (full width at half maximum, FWHM) pulse at 1·06 $\mu$m wavelength was used. The laser beam was focussed on the target using an aspheric lens of focal length 10 cm. The targets were irradiated inside an evacuated chamber ($10^{-5}$ torr). The target could be moved perpendicular to the laser beam so that for each laser shot a fresh portion of the target surface was exposed without disturbing the laser beam focussing conditions. The minimum laser spot diameter at the focussed beam waist was 30 $\mu$m (FWHM). This was determined by photographing the intensity distribution using an identical lens on an IR sensitive film (Kodak 4143). Figure 1 shows the experimental set-up schematically. The radial intensity distribution in the focal plane is also shown in the inset of the figure. The laser spot diameter on the target was varied by moving the target into the near field of the focussing lens while the incident laser intensity was varied by attenuating the laser beam using suitable neutral density filters.

Both single and double foil targets were used. Single foil targets were made of a 6 $\mu$m thick plastic foil. For double foil configuration, a 2 $\mu$m thick aluminium impact foil was placed behind a 6 $\mu$m thick plastic target foil. Separation between the target and impact foils was varied between 100 and 200 $\mu$m. Double foil configuration is more preferable so that the error caused by the low density matter on the rear side of the target foil is eliminated. This low density matter also casts a shadow as a result of which the motion of the high density matter is obscured. An impact foil placed behind the target foil reacts only when the high density accelerated matter makes an impact on it. If the two foils are separated by a distance large enough so that the target foil makes an impact after the initial acceleration phase is over, the impact time data and foil separation can yield the velocity of the target foil. The probe beam (0·53 $\mu$m wavelength) was derived from the main laser which ensured an easy synchronization of the probe pulse and main laser pulse. For this, a fraction of the 1·06 $\mu$m beam was temporally shortened and the

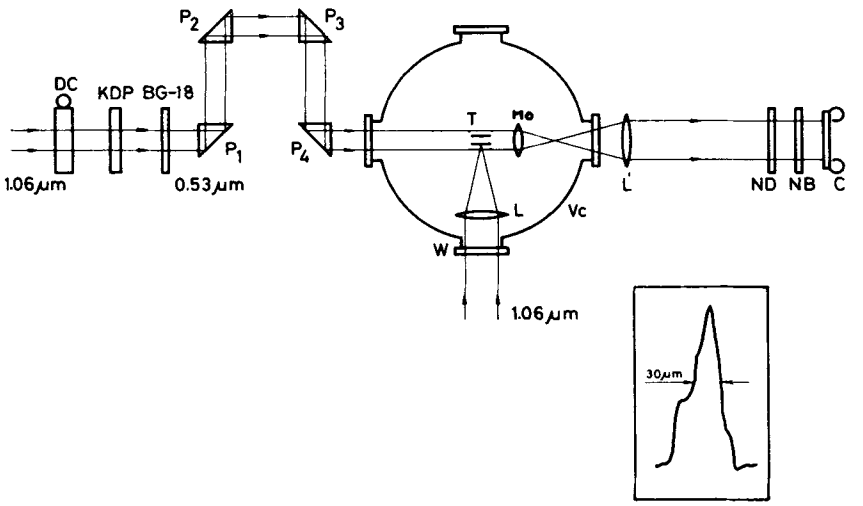


**Figure 1.** Experimental set up. T-Target foils, L-Focussing lens, W-Window, Vc-Vacuum chamber, Mo-Microscope objective, L'-imaging lens, ND, NB-Filters, C-Camera, DC-Saturable absorber cell, KDP-KDP crystal for second harmonic generation, BG-18-Green filter to cut off residual 1·06 $\mu$m beam, $P_1$, $P_2$, $P_3$, $P_4$–Folding prisms for optical delay.

frequency up converted into its second harmonic (0·53 $\mu$m) in a type-1 phase matched KDP crystal. Energy and pulse duration (FWHM) of the probe beam thus generated, were 50 $\mu$J and 2nsec respectively. Image of the targets illuminated by the probe beam was obtained with an $f/2$ objective lens on a type 107 polaroid film to give a magnification of 15. The spatial resolution was 15 $\mu$m. A variable optical delay was introduced in the path of the probe beam, so that, the target behaviour could be recorded at any desired instant of time with respect to the peak of the main laser pulse. The shadowgrams of the unirradiated foil is shown in figure 2a whereas shadowgrams of the foil in motion at various instants of time are shown in figures 2b and 2c.

In the double foil configuration, the target velocity was determined from its time of flight to the impact foil placed at a known distance. The flight time was determined by noting the probe delay time at which the impact foil reacts to the collision with the accelerated target foil. The probe delay time has been defined as the time interval after which the peak of the probe arrives at the target after the peak of the main laser pulse. The reaction of the impact foil to the target foil's collision occurs when the dense part of the target foil rear reaches the impact foil. The target velocity can be determined by varying the target-impact foil separation and plotting it against the impact time for a fixed laser intensity. Figure 3 shows a typical plot of impact time *vs* target-impact foil separation. If the foils collide after the initial ablative acceleration phase is over, the plot is linear and the slope gives the final target velocity. This condition was reasonably satisfied in our experiments.

In single foil targets, velocity of the dark shadow of the foil's rear ejecta was determined by measuring the axial position of the ejecta edge at various instants. Figure 2d shows the shadowgram of a single 6 $\mu$m plastic foil in motion after being irradiated by a laser pulse of intensity $3{\cdot}5 \times 10^{13}$ W/cm$^2$. Slope of the plot of the axial position *vs* time gives the target velocity. Although the leading edge of such a shadow consists of

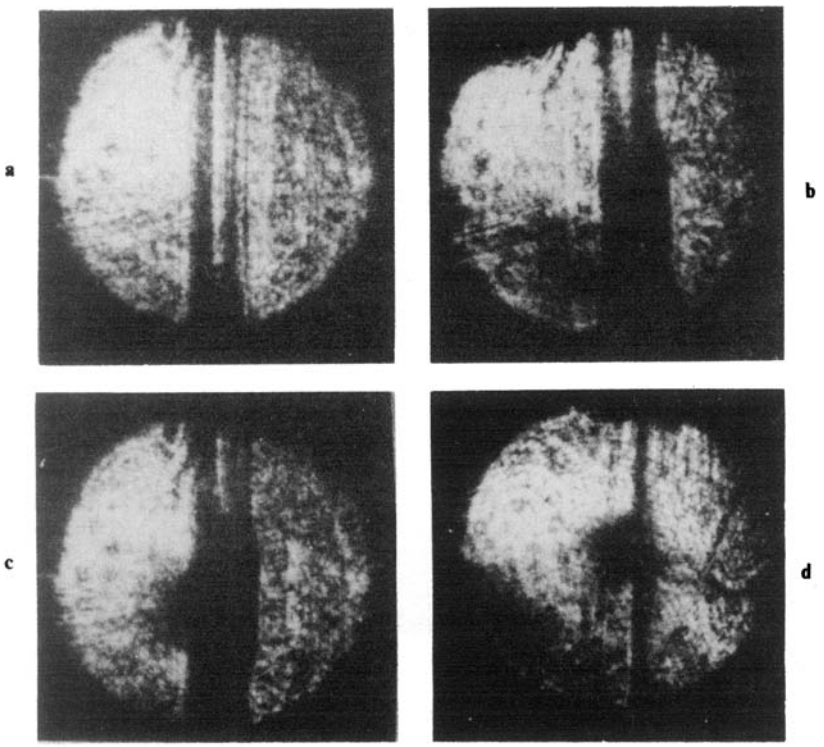


**Figure 2.** Shadowgram of the **a.** unirradiated foils, **b.** irradiated foils at the instant of impact of target foil on impact foil (3nsec probe delay), **c.** irradiated foils 3nsec after the impact (*i.e.*; 6 nsec probe delay), **d.** a single foil irradiated.

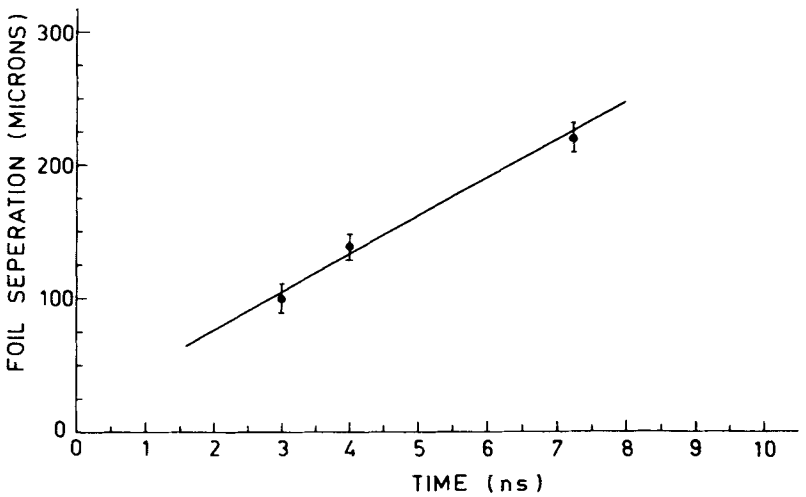


**Figure 3.** Impact time data to determine target foil velocity. Foil separation plotted against impact time.

low density material (Grun *et al* 1982), it has been shown that the dense target material also moves inside the rear dark shadow region at about the same velocity as that of the shadow edge (Stamper *et al* 1981). Thus this technique is also expected to provide a reasonable estimate of the target velocity. Our results also support this view.

## 3. Results and discussions

Ablation pressure $P$ was calculated using the relation $P = \rho tv/\tau$ where $\rho$, $t$ and $v$ are the target density, initial thickness and velocity respectively and $\tau$ is the irradiation time (Ripin *et al* 1980). Laser pulse duration has been taken as the irradiation time in our experiments. The value of the absorbed intensity at various levels of incident intensity was used from an earlier experiment (Sharma to be published). The variation of ablation pressure as a function of absorbed intensity for two different laser focal spot diameters *i.e.* 30 $\mu$m and 500 $\mu$m is shown in figure 4. For large spot irradiation, the pressure scales as $I_a^{0.7}$, where $I_a$ is the absorbed laser intensity. This scaling factor closely matches with the theoretical (Kidder 1968) and experimental (Grun *et al* 1982) values. It is interesting to note that the data from Naval Research Laboratory (Grun *et al* 1982) obtained using plastic foil targets and long (4nsec) laser pulses with a large focal spot (1mm diameter) irradiation falls very close to the extrapolated curve (a) shown in figure 3. In NRL experiments, lateral transport effects were minimised by making the laser plasma interaction area large. We, therefore conclude that our experiment with 500 $\mu$m diameter spot irradiation is also free from lateral transport effect. However, the ablation pressure scales as $I_a^{0.4}$ when a 30 $\mu$m spot is used for irradiation. This scaling is very much different from either the theoretically predicted or experimentally observed

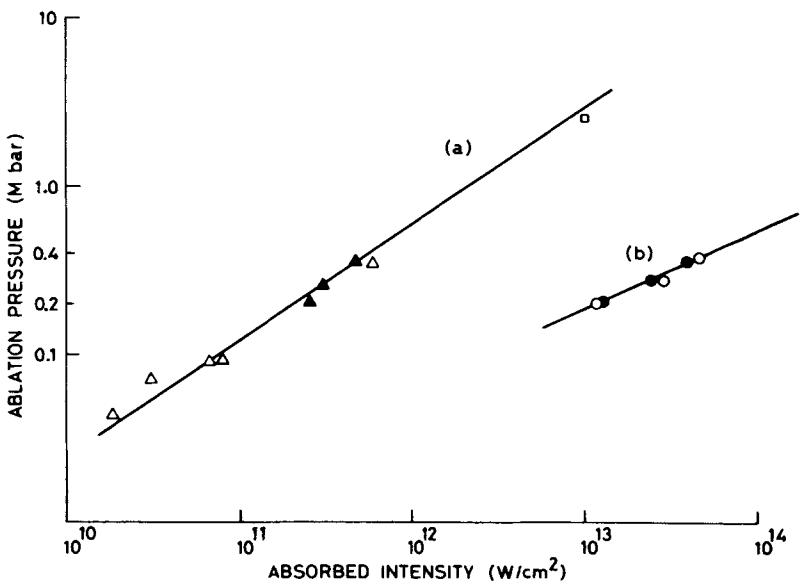


**Figure 4.** Scaling of ablation pressure with absorbed laser intensity **a.** for a focal spot of diameter of 500 $\mu$m and **b.** for a focal spot diameter of 30 $\mu$m. ▲, ●–Results of double foil experiments. Δ, O–Results of single foil experiments. □ – A data point corresponding to NRL experiments.

value when a larger target area is irradiated (Grun *et al* 1982). The lower scaling can be understood in terms of reduced irradiance due to lateral transport losses. It has also been shown that the plasma ablation velocity is greatly affected, when a small focal spot irradiation is used for experiments (Pant *et al* 1984). It has been shown in an earlier experiment (Sharma *et al* 1983) that the effective absorbed intensity $I_{\text{eff},a}$ due to lateral transport losses scales as $I_a^{0.5}$. Considering $I_{\text{eff},a}$ as the true intensity causing ablation, the pressure should scale as $I_{\text{eff},a}^{0.8}$. This modified scaling is very close to the one obtained when lateral transport effects are taken to be negligible (Lewis *et al* 1982; Grun *et al* 1982; RL-81-040, 1981). Thus a slower scaling for a small spot irradiation can be explained if we take into account losses due to lateral transport. On the other hand when a large spot diameter (*i.e.* 500 $\mu$m) irradiation is used, the fractional increase in the ablation diameter is negligible and therefore, no measurable reduction in the intensity is caused. This effect has been observed by other authors also while studying variation of plasma expansion velocity as a function of laser focal spot diameter (Grun *et al* 1981). To investigate this effect further we have examined one of the irradiated double foil targets in more detail. In this experiment, the laser intensity and focal spot diameter at the target foil were $5{\cdot}25 \times 10^{13}$ W/cm$^2$ and 30 $\mu$m respectively. Figures 2b and 2c are the shadowgrams recorded at an instant of time 3nsec and 6nsec after the peak of the main laser pulse respectively. As can be seen from figure 2b, the impact time is 3nsec for a 100 $\mu$m spacing between the foils. The velocity of the foil from figure 3 is found to be $3 \times 10^6$ cm/sec. The corresponding ablation pressure is 0·36 Mbar.

At an incident intensity of $5{\cdot}25 \times 10^{13}$ W/cm$^2$, the measured absorbed laser intensity is $3{\cdot}7 \times 10^{13}$ W/cm$^2$. This value is based on energy balance experiments conducted earlier. The ablation pressure determined in our experiments is found to be more than an order of magnitude less than that reported by others authors (Obenschain *et al* 1982) at similar absorbed intensity, however, with a larger 1 mm diameter laser spot size. These authors have assumed nearly insignificant lateral transport losses due to the larger laser spot irradiation. This assumption however, need not be true in our experiments where the irradiation spot diameter was only 30 $\mu$m (FWHM). A decrease in the laser irradiance due to foil motion away from the focal plane during irradiation would not explain the observed lower pressure. It is so, because, the laser spot diameter at a distance of 100 $\mu$m away from the waist of the beam is about 50 $\mu$m. Thus, a reduction in the laser intensity on the target due to its motion is not very significant. We therefore feel that a significant lateral transport of energy from the laser focal spot region is responsible for the observed lower pressure. A further evidence of lateral energy transport can be seen from figure 2c. This shadowgram was recorded 3nsec after the impact. It clearly shows that the diameter over which the impact foil has moved is much larger than the laser spot diameter on the target foil. The transverse dimensions of the accelerated impact foil at its half opacity points is about 150 $\mu$m. Since the shadowgram has been recorded 3nsec after the impact, we can expect the entire accelerated target foil to have collided and moved the impact foil. The diameter of the impact foil ejecta thus should correspond to the diameter of the accelerated foil which means that the actual ablation diameter of the target foil corresponds to the diameter of the ejecta of the impact foil. A similar (165 $\mu$m) transverse hot thermal plasma diameter (FWHM) due to lateral transport has also been observed in an earlier experiment, conducted using a pinhole camera, under similar experimental conditions (Sharma to be published). When the laser focal spot diameter (30 $\mu$m) is replaced by 150 $\mu$m (the actual ablation diameter) the effective absorbed irradiance on the target comes out to be

$1{\cdot}5 \times 10^{12}$ W/cm$^2$ instead of $3{\cdot}7 \times 10^{13}$ W/cm$^2$). This therefore, should be the effective absorbed intensity responsible for the ablative acceleration of the target foil. An ablation pressure of 0·4 Mbar was found at an intensity of $10^{12}$ W/cm$^2$ by Obenschain *et al* (1982). This value is close to the effective irradiance of $1{\cdot}5 \times 10^{12}$ W/cm$^2$ in our experiments for about the same ablation pressure (0·36 Mbar). Thus, lateral transport of energy beyond the irradiated spot region appears to reduce the effective irradiance causing a lower ablation pressure than expected from theory.

We have also tried to estimate the extent of the target heated due to lateral energy transport using the classical thermal conduction formula (Dawson 1970). The thermal conduction length according to the formula can be written as

$$l = (\eta t/c_v)^{1/2}, \tag{1}$$

(where $\eta$(thermal conductivity) $= (5{\cdot}85 \times 10^{12} \times T^{5/2})/Z(\ln \Lambda)$ ergs/sec. deg. cm (2)

and

$c_v$ (specific heat) $= 2\ (n_e + n_i) \times 10^{-16}$ ergs/cm$^2$·deg

Since $n_e = Zn_i$

$$c_v = 2n_e\left(\frac{1}{Z} + 1\right)^{-1} 10^{-16} \text{ ergs/cm}^2 \text{ deg} \tag{3}$$

In (2) and (3) $T$ is the electron temperature, (0·5 keV in our experiments) $Z$ the average atomic number (2·6 for polyethylene), ($\ln \Lambda$) = Coulombic logarithm (7 for 0·5 keV) and $n_e$ = electron density at critical surface ($10^{21}$ ele/cc for Nd:glass laser.) The parameter $t$ is the time that a density element, from which heat is conducted, spends in the region of interest before spreading out. (Lewis *et al* 1982) and is given by

$$t = L/c_s \tag{4}$$

where $L$ is the density scale length at the critical density surface (which can be considered to be equal to the focal spot diameter) and $c_s$ is the sound velocity given by

$$c_s = (ZKT/M)^{1/2} \tag{5}$$

where $M$ is the ion mass. Substituting these relations in (4), for $T = 0{\cdot}5$ keV, we get $t = 0{\cdot}17$ nsec. Further, using this value of $t$ in (1), and substituting for $\eta$ and $c$ from (2) and (3), we get $l = 60$ $\mu$m. Then, for a focal spot diameter ($D_f$) equal to 30 $\mu$m the diameter of the spot heated by thermal conduction (i.e. ablation diameter $D_a$) is equal to $(2l + D_f)$ $\mu$m. This value agrees well with our experimental findings. Shadowgrams taken at a large delay (figure 2c) shows the diameter of the rear foil ejecta to be 150 $\mu$m which corresponds to the ablation diameter.

The probe pulse duration of 2nsec used by us is larger than that used by others (Stamper *et al* 1981; Grun *et al* 1981) where, generally, a 100–300 psec pulse is used. Hence, a certain amount of error in the estimation of rear target velocity and ablation pressure can be expected. In our experiments therefore, a maximum error of 1 nsec is possible in the determination of the impact time. Then, the calculated pressure does not vary more than 25% and so still remains far less than that obtained under conditions of no lateral transport (Obenschain *et al* 1982). In other words, any error due to a finite duration of the probe pulse in our experiments cannot explain an order of magnitude difference in the measured ablation pressure.

In conclusion, we can say that the ablation pressure scaling with absorbed intensity is

greatly affected by the laser focussing conditions. Small spot irradiation shows a slower scaling as compared to a larger spot. The difference in scaling can be explained if lateral transport losses are considered. Difference between the expected and measured ablation parameters like target velocity and ablation pressure can be explained if an effective, rather than the actual absorbed intensity is considered.

## Acknowledgements

The authors wish to acknowledge the help rendered by the high power laser team by making available the Nd: glass laser facility for these experiments.

## References

Bruckner K and Jorna S 1974 *Rev. Mod. Phys.* **46** 325
Dawson J M 1970 *Laser Plasmas and nuclear energy* (ed) H Hora (New York: Plenum Press) 1975
Grun J, Decoste R, Ripin B H and Gardner J 1981 *Appl. Phys. Lett.* **39** 545
Grun J *et al* 1982 *Phys. Fluids* **26** 588
Kidder R E 1968 *Nucl. Fusion* **8** 3
Lewis C L S *et al* 1982 *J. Phys.* **D15** 69
Nishimura H *et al* 1981 *Appl. Phys. Lett.* **39** 592
Nuckolls J, Wood L, Thiessen A and Zimmerman G 1972 *Nature* (London) **239** 139
Obenschain S P *et al* 1982 NRL Report 4747
Pant H C, Sharma S and Shirsat T S 1984 *J. Appl. Phys.* **55** 697
Raven A *et al* 1982 *Appl. Phys. Lett.* **40** 776
Ripin B H *et al* 1980 *Phys. Fluids* **23** 1012
RL-81-040, 1981 Rutherford Laboratory Central Laser Facility Annual Report
Sharma S, Pant H C and Moncet M 1983 *J. Appl. Phys.* **54** 4666
Stamper J A *et al* 1981 *Laser interaction and related plasma phenomena* (ed.) H J Schwarz M J Lubin and B Yaakobi (New York: Plenum Press) **5** 617
Van Kessel C G M 1975 *Z. Naturforschung.* **30** 1582